MERCURY CADMIUM TELLURIDE FOR HIGH OPERATING TEMPERATURE INFRARED DETECTORS

R. Ashokan*, T. S. Lee, J. Zhao, Y. Chang, and S. Sivananthan
MicroPhysics Laboratory, Department of Physics
University of Illinois at Chicago
845 W. Taylor street, Chicago, IL 60607

P. S. Wijewarnasuriya, Y. Chen, G. Brill, and N. K. Dhar
Army Research Laboratory
2800 Powder Mill Road, Adelphi, MD 20783-1197

ABSTRACT

High Operating Temperature (HOT) Infrared detectors are required for upgrades of existing Army systems such as the AN/TAS-4 and also for Future Combat Systems. The higher operating temperature for the infrared photon detector could be achieved by suppressing the thermally generated noise. Non-equilibrium mode of operation is an approach to achieve HOT infrared detectors. In this paper, we demonstrate two important milestones that are critical for the development of HOT infrared detectors. First, the growth of high quality (minority carrier lifetime of 7.2 μsec at 200K) heterostructures based on mercury cadmium telluride by molecular beam epitaxy for equilibrium and non-equilibrium types of detectors. Secondly, the fabrication of p on n format photovoltaic infrared detectors with very high impedance (R_0A) on the order of high 10^8 Ohm-cm^2 at 80K are illustrated.

1. INTRODUCTION

The narrow band gap semiconductor, mercury cadmium telluride (HgCdTe) has been widely used to produce state-of-the art infrared imaging devices in both 3-5 μm and 8-14 μm atmospheric windows. At present, these detector arrays are cooled to cryogenic temperatures to suppress the thermal generation of carriers in order to achieve maximum sensitivity and detectivity. The weight, cost and reliability problems associated with the cooling mechanism have limited the application potential of these devices. For infrared detection near room temperature, GaAs photocathode image intensifiers (visible to <900 nm) have been improved to give background-limited performance (BLIP) at the extremely low light levels. Uncooled thermal detector arrays based on pyroelectric or bolometric principles now have sensitivities of a few 10's of mK. Due to the intensive research effort, in the past two decades, HgCdTe infrared detector arrays can now be tailored in different wavelength range from 1-14 μm. The sensitivity of these devices is better than the GaAs based image intensifiers. The noise equivalent temperature difference (NETD) of cooled HgCdTe is much better than the bolometric and pyroelectric imaging arrays. Moreover, for applications requiring high frame rates, fast response and longer range, photon detectors that are inherently more sensitive and faster than the thermal detectors are required. The HgCdTe detector is an intrinsic photon detector and absorbs the infrared radiation across the fundamental energy gap. Hence, the HgCdTe based detectors possess higher optical absorption coefficient, quantum efficiency and low thermal generation rate than the extrinsic detectors and silicide Schottky-barrier type of devices. Therefore, the operating temperature of HgCdTe based detectors could be higher compared to other types of photon detectors. The main obstacle in achieving this goal is the large level of noise due to Auger generation and recombination near room temperature. Ashley et al. (1986) proposed to suppress the Auger process by reducing the electron and hole concentrations below their equilibrium values, since the Auger cross-section is proportional to the square of the carrier concentration. Carrier exclusion in photoconductive devices and carrier extraction in photovoltaic devices have been employed (Jones et al., 1998) to demonstrate this concept. These devices require multilayer structures with well-controlled doping profiles. The MBE technique with demonstrated flexible manufacturing capability (Bajaj, 2000) and precise control over the material composition, doping and multilayer growth capability is best suited for the growth of such advanced device structures. In this paper, we report the growth of high quality n-HgCdTe absorber layers on 3-inch diameter silicon substrates by MBE, followed by the growth of non-equilibrium format heterostructures on CdZnTe substratres. High performance p on n equilibrium format devices at 80K are demonstrated that form the basis for the growth and fabrication of advanced HOT structures and devices. After establishing this baseline device process, we grew non-equilibrium format heterostructures on lattice-matched CdZnTe(211)B substrates and fabricated high performance p+nn+ format devices. Excellent zero-bias impedances (R_0A) are demonstrated both in p+/n (R_0A=

Report Documentation Page

1. REPORT DATE	2. REPORT TYPE	3. DATES COVERED
00 DEC 2004	**N/A**	**-**

4. TITLE AND SUBTITLE		5a. CONTRACT NUMBER
Mercury Cadmium Telluride For High Operating Temperature Infrared Detectors		5b. GRANT NUMBER
		5c. PROGRAM ELEMENT NUMBER
6. AUTHOR(S)		5d. PROJECT NUMBER
		5e. TASK NUMBER
		5f. WORK UNIT NUMBER

7. PERFORMING ORGANIZATION NAME(S) AND ADDRESS(ES)	8. PERFORMING ORGANIZATION REPORT NUMBER
MicroPhysics Laboratory, Department of Physics University of Illinois at Chicago 845 W. Taylor street, Chicago, IL 60607; Army Research Laboratory 2800 Powder Mill Road, Adelphi, MD 20783-1197	

9. SPONSORING/MONITORING AGENCY NAME(S) AND ADDRESS(ES)	10. SPONSOR/MONITOR'S ACRONYM(S)
	11. SPONSOR/MONITOR'S REPORT NUMBER(S)

12. DISTRIBUTION/AVAILABILITY STATEMENT
Approved for public release, distribution unlimited

13. SUPPLEMENTARY NOTES
See also ADM001736, Proceedings for the Army Science Conference (24th) Held on 29 November - 2 December 2005 in Orlando, Florida. , The original document contains color images.

14. ABSTRACT

15. SUBJECT TERMS

16. SECURITY CLASSIFICATION OF:			17. LIMITATION OF ABSTRACT	18. NUMBER OF PAGES	19a. NAME OF RESPONSIBLE PERSON
a. REPORT **unclassified**	b. ABSTRACT **unclassified**	c. THIS PAGE **unclassified**	**UU**	**8**	

6×10^8 Ohm-cm^2, cut-off=5.1 μm at 80K) and p+/n/n+ format devices (R$_0$A= 10^7 Ohm-cm^2, cut-off=6.4 μm) at 80K that serve as the key milestones in the development of HOT infrared detectors.

2. BRIEF REVIEW OF THE NON-EQUILIBRIUM CONCEPT AND REQUIREMENT

Noise in a photon detector is due to a combination of internal processes such as Auger, Shockley-Read-Hall, and radiative recombinations, together with external background photon noise. To achieve high device performance at or near room temperature, the thermally activated internal generation processes need to be reduced to an insignificant level, i.e., to reduce the device noise to the background level. The non-equilibrium operation is one way to meet this objective. The basic concept is a two terminal excluded/extracted device. The central region of the device, where the radiation is to be absorbed in an infrared detector, is near intrinsic and is ν−type (lightly doped n-type) or π−type (lightly doped p-type) and is sandwiched between two layers that form the excluding and extracting contacts with the absorber layer. One of these layers could be a wide gap n$^+$ layer, such that the Fermi energy is high in the conduction band. The other layer could be a wide gap p-type layer. Under reverse bias and at temperatures where the absorber region is near intrinsic, minority carrier extraction occurs at the diode junction resulting in large reductions in the minority carrier densities in its vicinity. The isotype junction (n ν) forms an excluding contact to the central region, thus preventing the injection of carriers to replace those removed at the diode junction, so the minority carrier density drops by several orders of magnitude throughout the absorber region. The majority carrier concentration also falls, to keep space charge neutrality, from the equilibrium intrinsic level to the extrinsic value. The net decrease in the carrier density below its equilibrium value results in drastic reduction in the dark current enabling the device to operate at higher temperatures.

From the Auger recombination time point of view (τ_{A7} −Auger7 process in p-HgCdTe and /τ_{A1} Auger1 process in n-HgCdTe), the use of P-π-N$^+$ heterostructure is advantageous because $\gamma = \tau_{A7}/\tau_{A1}$ is higher than unity (γ =3~6 for Hg$_{1-x}$Cd$_x$Te over the range x = 0.16~0.40 and T = 50~300K,) and the detectivity can be improved by a factor of $\gamma^{1/2}$. Whereas, practically, p-type HgCdTe layer has higher density of Shockley-Read recombination centers resulting from Hg-vacancy, which might make it harder to get the benefit of longer lifetime of τ_{A7}. On the other hand, the growth of high quality n-HgCdTe layers with low SRH centers, low electron concentration is relatively easier. Low carrier concentration in the absorber is a key requirement in order to reduce it further

under non-equilibrium operation so as to suppress the Auger recombinations in the LWIR-HgCdTe that in turn facilitates higher operating temperatures. Such low nonequilibrium carrier concentrations have been recently achieved by the Elliot group (Elliot et al., 1996) in 9 μm bulk HgCdTe at 295 K. Furhtermore, theoretical calculations of the impact of band structure engineering, photon recycling and carrier depletion as a function of detector temperature on photon detectors have been previously performed by Grein and Ehrenreich (1997). The other requirements include proper design of the interface gradients to maintain a good carrier dynamics and doping level and thickness of the p and n+ layers. The absorber layer should be thinner than a diffusion length, yet thick enough for IR absorption. The bottom n$^+$ and p$^+$ layers should be of wider band gap than the absorber layer. Also, the n$^+$ exclusion layer should be thick enough, at least 3 times the minority carrier diffusion length, to prevent minority carrier injection from this layer.

To achieve p+n-n+ type devices, it is necessary to establish the processes for p+n format devices, so that the key process parameters are standardized. In the following section, we describe the growth of two types of heterostructures employed in this study.

3. HETEROSTRUCTURES GROWN BY MOLECULAR BEAM EPITAXY (MBE)

In this study, our goals were to (i) achieve high impedance p+n format detectors based on n-type heterostructure grown on 3-inch diameter CdTe/Si substrates, and (ii) apply the knowledge gained in step (i) to design and grow HOT detector structures on lattice matched CdZnTe substrates. The growth of HOT detector structures requires careful control over HgCdTe composition profiles, layer thickness, and n-type doping levels. Before the growth of "HOT" detector structures, calibration layers were grown to calibrate the composition, growth rate and doping level of the HgCdTe material, followed by the growth of HgCdTe heterostructures on silicon substrates to establish the baseline process by fabricating p+n format devices. A schematic of the structure grown to establish the baseline processes for high performance p+n format equilibrium devices is shown in Fig.1a and that for the non-equilibrium format structure is shown in Fig.1b. The heterostructure shown in Fig.1a was grown on 3" CdTe/Si substrates prepared by in Army Research Laboratory, whereas the structure shown in Fig.1b was grown on lattice-matched CdZnTe (211)B substrates. The front side polished CdZnTe (211)B substrates with a Zn mole fraction of 3.5±1.0% were purchased from Nikko Materials USA, Inc.

CdTe t=0.03 μm
MW MCT t=0.29 μm
x-graded, t= 0.07 μm
MW x=0.3 MCT t=10 μm
SW MCT t= 0.5 μm
VLWIR MCT t=0.05 μm
HgTe/CdTe SL x10
(211)B CdTe/Si

(a)

CdTe t=0.03 μm
widegap MCT, x=0.38 t=0.29 μm
x-graded, t= 0.2 μm
MW x=0.3 MCT t=5-8 μm
x-gradient MCT t= 0.9 μm
N+ MWIR MCT t=3.1 μm
VLWIR MCT t=0.05 μm
HgTe/CdTe SL x10
(211)B CdZnTe

(b)

Fig. 1. Schematic of the layer structure for (a) n-HgCdTe/CdTe(211)B/Si heterostructure growth by MBE for p+n devices and (b) the non-equilibrium format structure on CdZnTe(211)B substrates.

The CdTe/Si surface appeared smooth and mirror-like. The HgCdTe epilayers were grown in a Riber 32P MBE system equipped with high energy electron diffraction (RHEED), an 88-wavelength spectroscopic ellipsometer, a pyrometer and a Hg valved cell. Solid CdTe and Te were used as source materials. Elemental indium was used as the n-type dopant. The Microphysics Laboratory at the University of Illinois pioneered the growth of CdTe and HgCdTe on silicon substrates (Sporken, 1989; Sivananthan, 1995).

Before the growth, the substrates were chemically cleaned using isopropyl alcohol, acetone and methanol, etched in bromine/methanol, and rinsed in methanol and deionized water. Then, the substrates were dried and mounted on an indium-free molybdenum holder with a graphite thermal diffuser plate at the backside. Once introduced into the growth chamber, excess Te present on the sample surface was stripped at 250°C, and CdTe was deposited to reduce the surface roughness. *In-situ* SE and RHEED were used to monitor the oxide desorption, interface formation and growth together with the substrate thermocouple. The pyrometer was used to help monitor the substrate temperature. The composition in each layer and the graded interface between the layers are critical for efficient performance of the device. This was monitored during the growth by in-situ spectroscopic ellipsometry (SE). A SE with a rotating analyzer that can measure 88 wavelengths in the range from 1.6 to 4.3eV (the Woollam M88) was used here. The evolution of the dielectric function during the substrate preparation and the HgCdTe growth procedures were recorded in real time. Optical models were set up to fit the experimental data in order to determine parameters of interest such as surface roughness and optical constants (which are related to HgCdTe layer compositions). Two parameters, composition and surface roughness, are obtained from the ellipsometry measurements and plotted in Fig. Here, Fig.2(a) is a representative SE data for equilibrium type structures whereas Fig.2(b) is that for a non-equilibrium type structure. The substantial differences in the compositional profile along the growth direction between the two types of structures grown are clearly seen in Fig.2. The bottom layer of the HOT detector structure was indium-doped to produce an n+ layer, whereas the three layers above were undoped or low level n-type doped. During the growth, the CdTe temperature was intentionally ramped up/down 10°C for 3 minutes to produce compositional gradients between the narrower bandgap layers (lower composition) and the wider bandgap layers (higher composition).

After the growth, the Cd mole fraction and subsequently the cutoff wavelength of the layers were measured by room temperature Fourier transform infrared (FTIR) transmission measurements. The FTIR for a representative sample are shown in Fig 3(a) and 3(b) for the equilibrium type and non- equilibrium type structure, respectively. The Cd mole fraction in Fig. 3(a) was measured to be 0.305 from the wavelength corresponding to 50% of transmission maximum that will be equivalent to 5 μm cut-off at 80K. On the other hand, due to the several HgCdTe layers in the HOT detector structure, the cutoff edge is relatively more sloped and not very sharp when compared with monolayers (for example Fig.3a).

The as-grown layers were then annealed to fill the Hg vacancies in the HgCdTe layers. The annealing parameter is carefully chosen to fill the Hg vacancies as well as to activate the dopants. Usually, a two or three – step annealing procedure is adopted. A quartz ampoule with a tube insert to prevent residues from the sealing process is used here. The tube is divided into two compartments with constriction in between. The Hg source remains in the bottom compartment while the sample remains in the top compartment. The tube is evacuated, back-filled with argon and sealed. The annealing is then carried out in a two-zone furnace with a
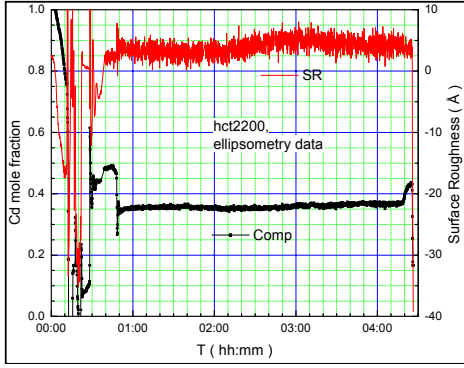
(a)
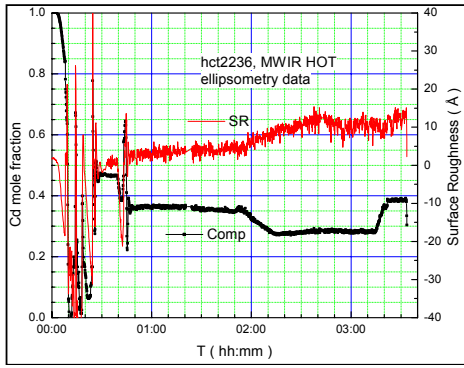
(b)

Fig. 2. The composition and surface roughness obtained from in-situ ellipsometry: (a) equilibrium format structure and (b) non- equilibrium format structure.

temperature difference of 5 to 10°C between the sample and the Hg source. The n-type annealing usually involves 235°C for 24 hours, while to activate the p-dopants as well as to fill Hg vacancies (for p on n device fabrication subsequently) a three step anneal involving 425°C for 10 minutes followed by 300°C for 4 hours and 235°C for 24 hours was found to produce the best device performance. The first step ensures proper site transfer for arsenic while the second step controls the junction formation and the third step ensures Hg-vacancy filling.

The carrier concentration and mobility in the absorber layers were obtained from the Hall measurements in Van der Pauw geometry, after chemically etching the top wide bang gap layers. The Hall characteristics of a non-equilibrium type sample are shown in Fig.4. The carrier concentration in the absorber layer is 3×10^{15} cm^{-3}. We believe that this could be further reduced (Shi et al., 1998) by a factor of 3 or more by optimizing the graded layer between the n+ contact layer and the absorber layer, in order to better meet the low carrier concentration requirements of non-equilibrium operation. It should be mentioned here that the absorber layer in the non-equilibrium format samples are grown on heavily n-doped (In) HgCdTe layers. Due to the memory effect, during the initial phase of the absorber

layer growth, the indium concentration will be somewhat higher than the set values.
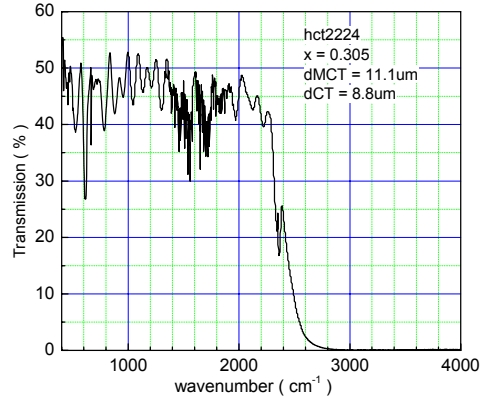
(a)
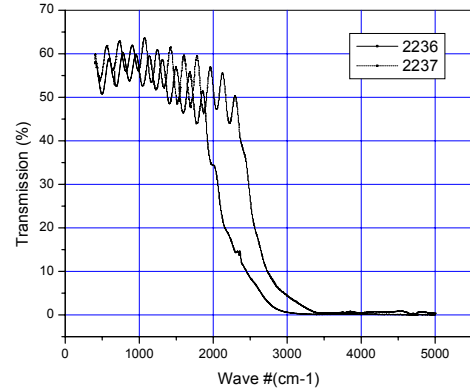
(b)

Fig. 3. (a) Room temperature FTIR of an equilibrium type structure and (b) non-equilibrium format structure (two samples are shown)
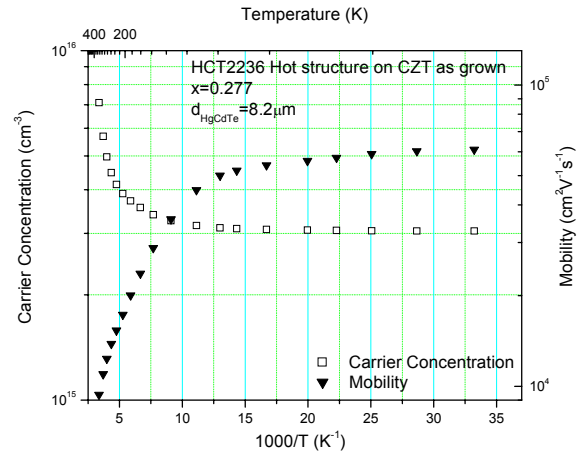
Fig. 4. The carrier concentration and mobility as a function of inverse temperature determined by Hall measurements on HCT 2236, a non-equilibrium format heterostructure grown on (211)B CdZnTe substrates.

4

4. ANALYSIS OF LIFETIME LIMITING RECOMBINATION MECHANISMS IN MWIR AND LWIR HOT DETECTORS

The source of noise or dark current as a function of operating temperature depends on the detector cut-off wavelength. In this section we compare the minority carrier lifetimes in MWIR and LWIR detectors predicted by theory. The minority carrier lifetime measured by photoconductive decay in the MWIR samples studied here are then compared with the theoretical predictions.

The interpretation of the experimentally measured lifetime of minority carrier in HgCdTe as a function of inverse temperature is normally done by parallel addition of the theoretical lifetimes due to three main mechanisms. These are radiative recombinations, Auger recombinations (Auger 1 process in n-HgCdTe and Auger 7 process in p-HgCdTe), and Shockley-Read-Hall (SRH) recombination mechanisms. The radiative process involves the direct band-to-band recombination of a conduction band electron with a heavy hole to emit a photon. The Auger-1 is believed to be the dominant recombination mechanism in n-type HgCdTe. This process involves the direct band-to-band recombination of a conduction band electron with a heavy hole and the excitation of another electron in the conduction band. The theoretical fitting was carried out by using the standard formulae for the three recombination processes.

The lifetime τ is computed as parallel addition of the SRH lifetime τ_{SRH}, Auger lifetime τ_A and radiative lifetime τ_R.

$$\frac{1}{\tau} = \frac{1}{\tau_{SRH}} + \frac{1}{\tau_A} + \frac{1}{\tau_R} \qquad (1)$$

The lifetime predicted by the theory is shown in Fig.5a for the MWIR HgCdTe case and in Fig.5b for the LWIR HgCdTe case. In both cases, Auger-1 curve is for n-HgCdTe absorber while the Auger-7 curve is for p-HgCdTe absorber. From Fig.5a, it is clear that the MWIR case, the benefit of non-equilibrium is minimal and the benefit if any can be observed only at temperatures > ~ 260K. This is because the radiative recombination is the limiting mechanism in the MWIR material at temperatures below 260K. This is a fundamental mechanism and is not influenced by the non-equilibrium operation. On the other hand, in the LWIR HgCdTe case shown in Fig.5b, irrespective of the conductivity of the absorber layer, significant advantage can be obtained by suppressing the Auger recombinations through non-equilibrium operation. However, as seen in Fig.5b, by suppressing the Auger-7 process dominant in the p-HgCdTe, better lifetimes can be obtained in comparison to suppressing Auger-1 in n-HgCdTe. For this reason, lightly doped p-HgCdTe

absorber is preferred over n-HgCdTe for LWIR non-equilibrium detectors.
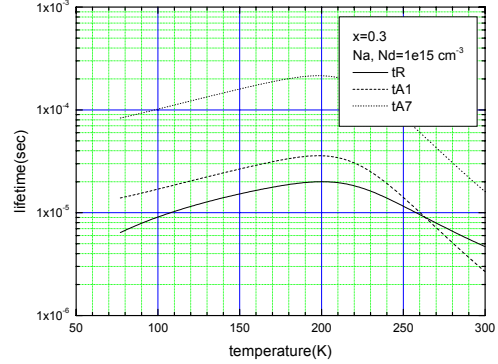
(a)
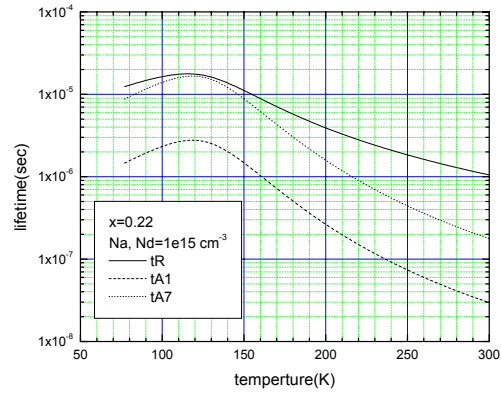
(b)

Fig. 5. Theoretical minority carrier lifetime as a function temperature for (a) n-MWIR HgCdTe and (b) LWIR HgCdTe. The radiative, Auger1 (n-type) and Auger 7(p-type) trends are shown by solid, dashed and dot lines respectively.
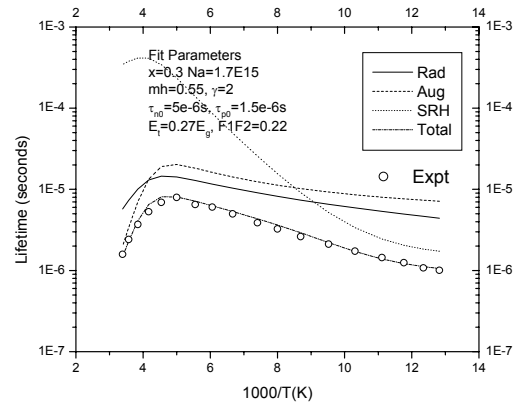
Fig. 6. The measured lifetime in n-HgCdTe based heterostructure after annealing. The fitting with theoretical model involving radiative, Auger, and SRH recombinations is also shown.

Minority carrier lifetimes of HgCdTe samples used here were measured by the photoconductive decay method. Test samples from the same wafer were used for the Hall and lifetime measurements. Care was taken to anneal these test samples along with the other parts of the wafer used for the subsequent device fabrication simultaneously to avoid variations if any. The measured minority carrier lifetime as a function of inverse temperature for an equilibrium type of structure discussed earlier is shown in Fig.6. This figure shows that excellent carrier lifetime of 7.2 µsec at 200K and 2 µsec at 80K in the n-HgCdTe absorber layer with 5 µm cut-off wavelength at 80K is achieved. The theoretical fitting discussed above is also shown in this figure. These results demonstrate that the lifetimes at higher temperatures are limited by radiative process as expected for MWIR material. At lower temperatures, the SRH seems to be the dominating mechanism. Further optimization of the growth parameters and/or annealing parameters could reduce the SRH defect density. However, at the operating temperatures expected for HOT detectors (>200K), this material structure is radiative-limited, which is a fundamental mechanism, thus exhibiting an excellent lifetime.

5. P ON N PHOTOVOLTAIC DEVICE FABRICATION AND MEASURED CHARACTERISTICS

Planar photovoltaic devices employing selective arsenic implantation for p-HgCdTe were fabricated on HgCdTe alloy-based heterostructures (p+n format) and HOT detector structures (p+nn+ format). The detectors with three different active areas of 40µmx40µm, 200µmx200µm, and 300µmx300µm were fabricated. The device passivation was done by CdTe grown in a MBE chamber. Arsenic ion implantation and a three step anneal mentioned earlier were used to obtain p on n type devices. The devices annealed with an additional intermediate step of 300^0C for 4 hours yielded the best I-V characteristics, presented later in this section. The device annealed with only the 425^0C and 235^0C steps and the devices with an additional 300^0C intermediate step but longer duration (8 hours) showed inferior I-V characteristics (higher dark currents) relative to the best device results presented later in this section. Those results are not included in this paper, for brevity. The spectral responses of the devices were measured using a NICOLET FTIR spectrometer. The detectors were wire bonded and mounted in a LN2 dewar for the testing.

The spectral response curves of a 300µm x 300µm device measured at 300K and 80K are shown in Fig.7(a) for the p+n format devices (HgCdTe/CdTe/Si) fabricated to establish the baseline process as described in Section-1. The curves are characterized by sharp cut-off. The wavelength at 50% of the maximum signal is defined as the cut-off wavelength. The 300K cut-off of this device is 4.2 µm while the 80K cut-off wavelength is 5 µm. This agrees very well with the Cd mole fraction measured by the in-situ ellipsometry as well as with the room temperature FTIR of this sample (discussed in the Section-3), demonstrating the excellent control over the composition of the material. Employing ellipsometry as the in-situ tool to monitor the composition real-time has tremendously improved the accuracy of the composition control in these materials. Similarly, the spectral response for a 300µm x 300µm device fabricated on a non-equilibrium format (HgCdTe/CdTe/Si) sample is shown in Fig..7(b). Here we observe soft spectral characteristics, may be due to a thinner absorber layer and or due to the higher composition contact layers on either side of the absorber layer. However, a relatively thinner absorber layer (4 to 6 µm) would suffice for full absorption at 180K operating temperature. Furthermore, the absorber layer thickness is optimized to yield good absorption but is less than the diffusion length at the required operating temperature of >200K for MWIR detectors.
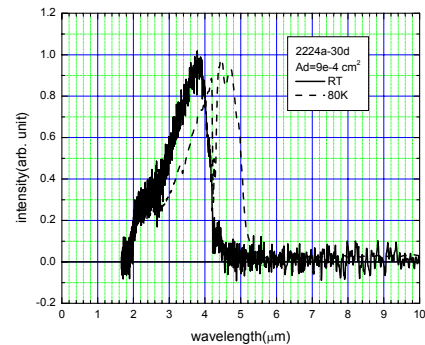

(a)
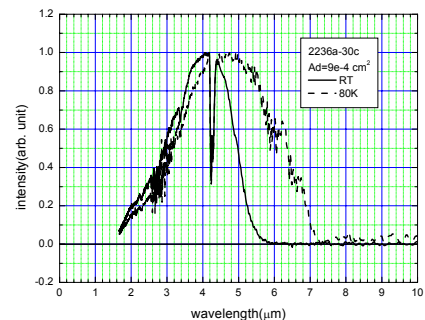
(b)

Fig. 7. The spectral response measured at room temperature and 80K in (a) a p on n device fabricated on MBE grown HgCdTe/CdTe/Si(211), (b) a device (p+n-n+) fabricated on a non-equilibrium format structure grown on CdZnTe(211)B substrate

The current-voltage measurements (I-V) were used as the primary characterization tool. The zero bias and reverse bias leakage currents characterize the performance of the p-n junction. The slope of the I-V curve at zero bias multiplied by the area of the detector defines the impedance of the device (R_0A) and is a figure of merit of the detector. The I-V measurements were carried out using a low temperature micro probe station from MMR Technologies. The devices were mounted on the cooling pad of the Joule-Thomson cooler and the chamber evacuated. Dry nitrogen at a typical pressure of 2000 psi is used to cool the samples and manual micromanipulators are used to contact the probes on the pads provided in each device. The pads are located well away from the active area to minimize the probability of damage due to the probing process itself.
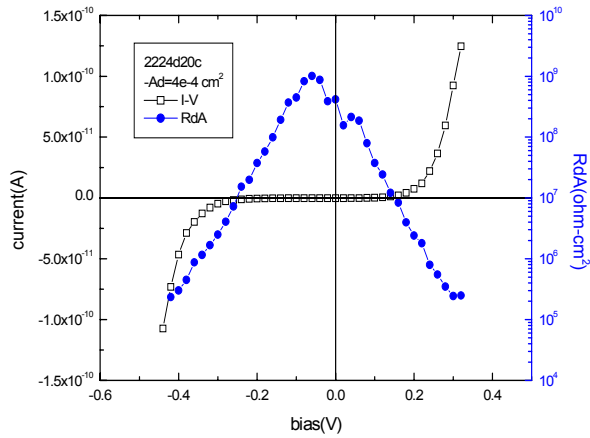
Fig. 8. The I-V and R_dA curves as a function of bias voltage for a 200μmx200μm active area diode fabricated on equilibrium-device type heterostructure (HgCdTe/CdTe/Si).
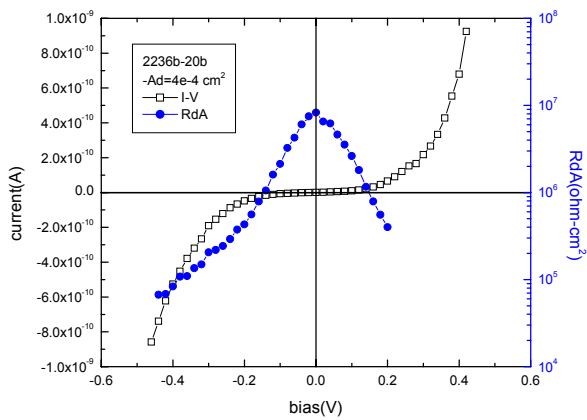
Fig. 9. The I-V and R_dA curves as a function of bias voltage for a 200μmx200μm area diode fabricated on non-equilibrium device type heterostructure (HgCdTe/CdZnTe).

The I-V characteristics representative of a good diode with 200 μm x 200 μm active area is shown in Fig.9. This p+n format device was fabricated on an equilibrium type of heterostructure (HgCdTe/CdTe/Si). The dynamic impedance (resistance-area product, R_dA) as a function of the bias voltage is also shown in this figure. Peak dynamic impedances on the order of 10^9 Ohm-cm^2 is observed in Fig.8, while the zero-bias resistance-area product (RoA) is around $6x10^8$ Ohm-cm^2. A comparison (not presented here) with 1-D theory show that these devices are g-r limited at 80K. These values compare well with the best results reported for devices on HgCdTe/CdZnTe and HgCdTe/CdTe/Si (Wijewarnasuriya et al., 1998).

The I-V characteristics of a similar active area device (p+n-n+) fabricated on a non-equilibrium type of heterostructure is shown in Fig. 9. The RoA value obtained here is on the order of 10^7 Ohm-cm^2. This is an excellent result considering that the cut-off wavelength of this device is 6.4 μm at 80K. The I-V and device impedance results from more devices on both formats are summarized in Table 1. More work is currently in progress to study their high temperature properties.

The leakage currents in the device originate from two main sources – (i) bulk and (ii) surface/interface-related. The currents from bulk material fundamentally consist of diffusion, generation-recombination and band-to-band tunneling currents. Ideally, these currents are a function of the material properties like, 'Cd' composition, doping concentration, and carrier lifetime. In practice, the material consists of defects that would lead to additional currents due to trap-assisted tunneling. The surface and interface related currents mainly originate from the defects on the surface of the material and the CdTe/HgCdTe interface. Improper passivation generates large fixed charges at the interface and fast and slow interface states that reduce the effective lifetime of carrier in the device leading to higher leakage currents. Generally, at zero-bias and small reverse bias region, the interface-related leakage currents dominate, while at larger reverse biases, the band-to-band (b-t-b) tunneling currents dominate. The I-V characteristics shown in Figs.8 and 9 show that the passivation-related leakage currents are minimal because at zero bias and small reverse biases, the dark current is very low (pA). On the other hand, at reverse biases > 300mV, the dark current increases with increasing bias, indicating contribution from b-t-b tunneling process. This corroborates with our earlier observation in Section-4 that at low temperatures (~80K), the SRH recombinations limit the lifetime. It may be possible that the defect levels introduced in the band gap due to the SRH centers are involved in promoting the b-t-b tunneling process at low temperatures.

Table 1. The devices fabricated and their key properties. Device active area: 40µmx40µm, 200µmx200µm, and 300µmx300µm.

S. No.	Device ID#	Device-spectral response	R_0A (Ohm-cm^2)		R_dA (Ohm-cm^2)	
		Cutoff Wavelength (µm) @80K	Mean	Highest	Mean	Highest
2224*	2224c	5.1	4.2e7	1.3e8	2.3e8	7.9e8
	2224d		9.2e8	1.9e9	1.8e9	3e9
2236**	2236b	6.4	6.0e6	8.3e6	1.5e7	2.3e7
2237**	2237b		1.5e5	1.5e5	1.8e5	1.8e5
2243**	2243b		9.0e5	9.0e5	1.0e6	1.0e6

*Equilibrium format devices on HgCdTe/CdTe(211)B/Si.

** Non-Equilibrium format devices on HgCdTe/CdZnTe (211)B.

SUMMARY

First, the baseline MBE grown HgCdTe device technology was established using n-HgCdTe based MWIR heterostructures grown on 3-inch diameter (211)B CdTe/Si. Excellent material characteristics including the carrier lifetime of 7.2 µsec at 200K and up to 2 µsec at 80K in the n-HgCdTe absorber layer with 5.1 µm cut-off wavelength at 80K were achieved. The photovoltaic detectors fabricated on these MWIR heterostructures show excellent zero-bias resistance-area product (R_0A) on the order of 10^8 Ohm-cm^2 and peak dynamic impedances on the order of 10^9 Ohm-cm^2.

Next, heterostructures suitable for non-equilibrium devices were grown on CdZnTe(211) substrates. Low leakage currents and high R_0A values 10^7 Ohm-cm^2 (cut-off wavelength 6.4 µm at 80K) were measured in these devices also. Further work is currently in progress to study the high temperature properties of the non-equilibrium format MWIR detectors and fabricate LWIR HOT detectors on MBE grown heterostructures.

ACKNOWLEDGMENTS

REFERENCES

Ashley, T., Elliott, C.T. and Harker, A.T. 1996: Non-equilibrium mode operation for infared detectors, *Infrared Physics* **26**, 303-315.

Bajaj, J., 2000: State-of-the-art HgCdTe infrared devices, *Proc. of SPIE*, vol. **3948**, 42-54.

Elliott, C.T., Gordon, N.T., Hall, R.S., Phillips, T.J. , White, A.M., Jones, C.L., Maxey, C.D. and Metcalfe, N.E., 1996: Recent Results on Metalorganic Vapor Phase Epitaxially Grown HgCdTe Heterostructure Devices, *J. Electron. Mater.* **25**, 1139-1145.

Grein, C.H. and Ehrenreich, H., 1997: Improvement of infrared detector performance in carrier depleted strained layer type II superlattices, *J. Appl. Phys.* **82**, 6365-6367.

Jones, C.L., Metcalfe, N.E., Best, A., Catchpole, R., Maxey, C.D., Gordon, N.T., Hall, R.S., Colin, T. and Skauli, T., 1998: Effect of Device Processing on 1/f Noise in Uncooled, Auger-Suppressed CdHgTe Diodes, *J. Electron. Mater.* **27**(6), 733-739.

Shi, X.H., Rujirawat, S., Ashokan, R., Grein, C.H. and Sivananthan, S., 1998: Ionization energy of acceptors in As-doped HgCdTe grown by molecular beam epitaxy, *App. Phys. Lett.* **73**, 638-640.

Sivananthan, S., Chen, Y.P., Wijewarnasuriya, P.S., Faurie, J.P., Smith, F.T. and Norton, P.W. 1995: Properties of $Hg_{1-x}Cd_xTe$ grown on CdZnTe on Si substrate, *Proc. 7 th Intl. Conf. on Narrow Gap Semiconductors,* 239-244.

Sporken, R., Sivananthan, S., Mahavadi, K.K., Monfroy, G., Boukerche, M., Faurie, J.P., 1989: Molecular beam epitaxial growth of CdTe and HgCdTe on Si (100), *Appl. Phys.Lett.* **55**, 1879-1881.

Wijewarnasuriya, P.S., Zandian, M., Edwall, D.D., McLevige, W.V., Chen, C.A., Pasko, J.G., Hildebrandt, G., Chen, A.C., Arias, J.M., D'Douza, A.I., Rujirawat, S., and Sivananthan, S., 1998: MBE P-on-n Hg1-xCdxTe Heterostructure Detectors on Silicon Substrates, *J. Electron. Mater.* **27**(6), 546-549.